Frequency-selective Heteronuclear Correlation (FS-HETCOR) Experiments in Solid-State NMR

Zhengfeng Zhang[1]*, Yongchao Su[2], Jun Yang[1, 3]*

1. National Center for Magnetic Resonance in Wuhan, Key Laboratory of Magnetic Resonance in Biological Systems, State Key Laboratory of Magnetic Resonance and Atomic and Molecular Physics, Wuhan Institute of Physics and Mathematics, Innovation Academy for Precision Measurement Science and Technology, Chinese Academy of Sciences, Wuhan 430071, P. R. China.
2. College of Pharmacy, The University of Texas at Austin, Austin, TX 78712, USA
3. Wuhan National Laboratory for Optoelectronics, Huazhong University of Science and Technology, Wuhan 430074, P. R. China

To whom correspondence should be addressed:
zhangzf@wipm.ac.cn (Z. Zhang)
yangjun@wipm.ac.cn (J. Yang)

Keywords
Heteronuclear correlation (HETCOR), Frequency-selective, Dipolar recoupling, Magic-angle spinning (MAS), solid-state NMR

Abstract

Heteronuclear correlation (HETCOR) is critical to obtain structural information in solid-state nuclear magnetic resonance (NMR). We propose novel frequency-selective Heteronuclear correlation (FS-HETCOR) experiments to selectively enhance the inter-atomic correlations of interest. FS-HETCOR relies on heteronuclear selective phase-optimized recoupling (SPRx), which is frequency-selective in heteronuclear recouping without using selective pulses. Compared to regular HETCOR, FS-HETCOR selectively enhances the desired heteronuclear correlations by a factor of up to 5 and suppresses the unwanted ones to 10% as demonstrated in ^{1}H-^{19}F and ^{1}H-^{13}C experiments under fast magic-angle spinning (MAS). Moreover, FS-HETCOR can theoretically be applied at arbitrary MAS rates by utilizing various SPRx schemes. We believe that the method will enhance the ability of solid-state NMR to probe heteronuclear structural information.

Introduction

Heteronuclear correlation (HETCOR) experiments play critical roles to obtain structural information in nuclear magnetic resonance (NMR).[1-5] Solid-state NMR often resorts to dipolar couplings that are 1-2 order of magnitude larger than scalar coupling to establish heteronuclear correlations. While magic-angle spinning (MAS) for line narrowing attenuates heteronuclear dipolar couplings, recoupling sequences are introduced to recover them for distance information.[6-17] Cross polarization (CP) is the most-widely utilized technique to establish ^{1}H-X or X-Y HETCOR experiments (X, Y = ^{13}C, ^{15}N, ^{19}F, ^{31}P, etc) in studies of proteins, catalysts, polymers, and pharmaceuticals.[18-25] However, most dipolar recoupling sequences often suffer from dipolar truncation[26], preferentially establishing correlations of strongly coupled nuclei. The correlations from distant nuclei are typically truncated and therefore difficult to be observed.

Frequency-selective homonuclear ^{1}H-^{1}H or ^{13}C-^{13}C correlations have been observed via selective phase-optimized recoupling (SPR)[27-28] and other pulse schemes[29-31]. They can provide considerable enhancements of the desired correlations as the polarization is deliberately transferred to a small population of nuclei with distinct resonance frequencies. Similarly, selectively-enhanced HETCOR may also be achieved via frequency-selective heteronuclear recoupling. However, to our best knowledge, current frequency-selective heteronuclear techniques are mostly applied to selective distance measurements[32-36], which rely heavily on selective pulses[37-41]. There is no known frequency-selective heteronuclear recoupling without using any selective pulses.

Methods

In this study, we propose a novel frequency-selective heteronuclear correlation (FS-HETCOR) experiment by employing heteronuclear selective phase-optimized recoupling (donated as SPRx). FS-HETCOR is designed to selectively observe and enhance the heteronuclear correlations of interest. Figure 1 shows the pulse sequences of SPRx-N_n (a) and corresponding FS-HETCOR experiments (b, c). SPRx is constructed by the unit of SPR that has been used for homonuclear recoupling[27], following the idea of our previous dual back-to-back pulses (DBP)[14-15]. The basic phases or super-cycled phases of SPRx-N_n are different on the two channels (see supplementary material).

Herein we demonstrate the usage of SPRx-4_1 and SPRx-4_3, which require the ν_1/ν_R ratios to be 2 and 0.75, respectively (ν_1 is the RF amplitude and ν_R is the MAS rate). The details in SPRx-4_1 and SPRx-4_3 are given in Table S1. For SPRx-4_1, the overall phases are (02132031 20310213 13203102 31021320)×90° and (02020202 20202020 13131313 31313131)×90° on channels ^{1}H and S, respectively. For SPRx-4_3, the overall phases are (02132031 20310213 13203102 31021320)×90° and (02020202 2020202 013131313 31313131)×90° on channels ^{1}H and S, respectively. Various SPRx-N_n schemes would exist for arbitrary MAS rates, similar to SPR that have been used under from slow to ultrafast MAS[27-28].

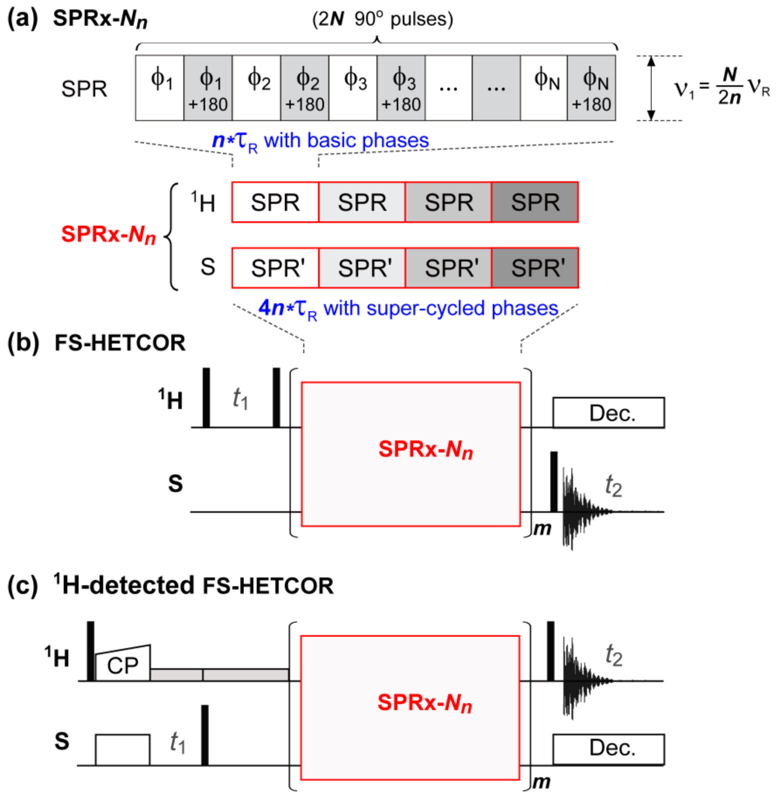

Figure 1 Pulse sequences of SPRx-N_n (a) and corresponding FS-HETCOR experiments (b, c). Original SPR-N_n consists of a block with N pairs of "$90°_{\phi_k}90°_{\overline{\phi_k}}$" and a repeated block with a 180 °phase shift, where ϕ_k represents the RF phase.[27] (a) The SPR unit with a length of $n\tau_R$ and basic phases is super-cycled to construct the heteronuclear SPR (SPRx), where τ_R is the MAS rotor period. The basic phases or super-cycled phases are different on the two channels (^{1}H and S). (b) In FS-HETCOR, SPRx-N_n is used for selective polarization transfer. Saturation pulses can be applied before the SPRx-N_n block on Channel S to suppress the unwanted signals. (c) The ^{1}H-detected FS-HETCOR is similar to CP-based heteronuclear single-quantum correlation (CP-HSQC)[42-46] but uses the SPRx block for selective S→^{1}H polarization transfer.

Results and discussion

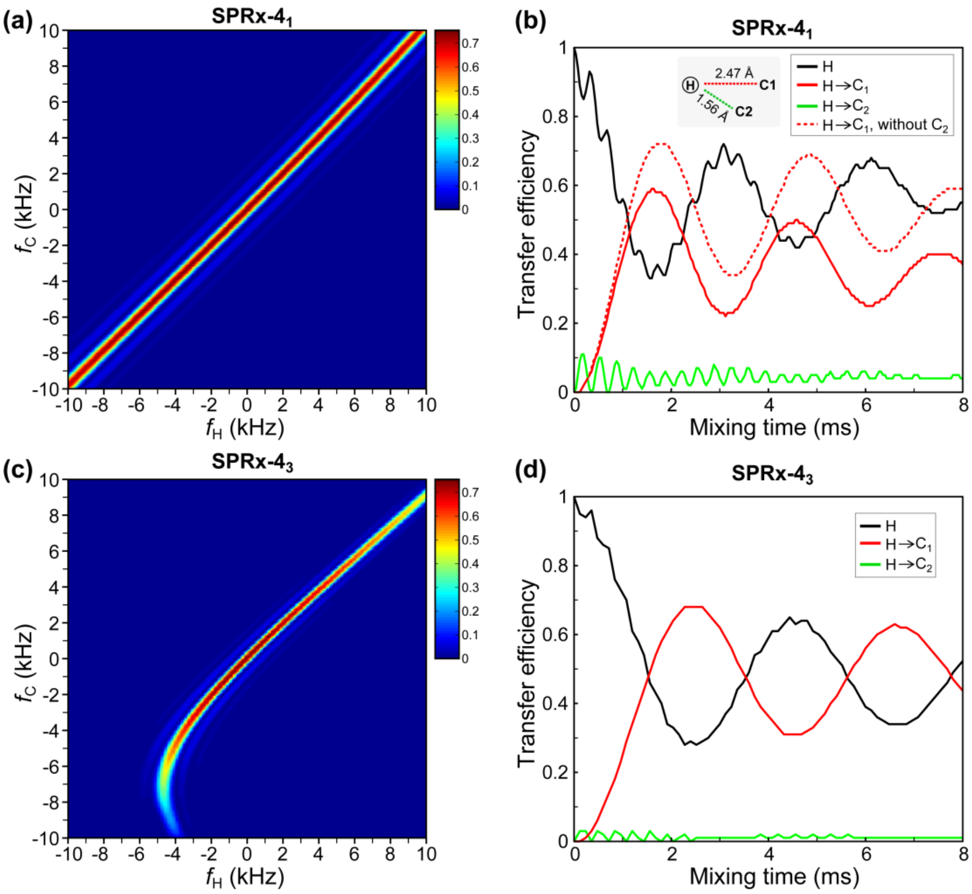

Figure 2 Simulated polarization transfer efficiency of $I_{z,\,H}$→ $I_{z,\,C}$ as functions of frequency offsets (a, c) and mixing times (b, d) of SPRx-4$_1$ and SPRx-4$_3$ under 100 kHz MAS. The RF amplitudes are 200 kHz ($2\nu_R$) and 66.7 kHz ($0.667\nu_R$) for SPRx-4$_1$ and SPRx-4$_3$, respectively. In (a, c), a two-spin system (^{1}H, ^{13}C) with the dipolar couplings of 2000 Hz is used. The f_H and f_C represent the frequency offsets of ^{1}H and ^{13}C$_1$, respectively. The mixing times are 1.68 ms (m = 42) and 2.4 ms (m = 20) for SPRx-4$_1$ and SPRx-4$_3$, respectively. In (b, d), a three-spin system (^{1}H, ^{13}C$_1$, ^{13}C$_2$) is used in simulations, with the dipolar couplings of ^{1}H-^{13}C$_1$, ^{1}H-^{13}C$_2$, and ^{13}C$_1$-^{13}C$_2$ being 2000 Hz, 8000 Hz, and 0 Hz, respectively. (^{1}H, ^{13}C$_1$) is on resonance and ^{13}C$_2$ is offset by 4 kHz. Simulations were performed under a magnetic field of ^{1}H 800 MHz by using the SIMPSON software[47].

Figure 2a and b show the simulated frequency-selectivity of SPRx-4$_1$ and SPRx-4$_3$, respectively. Efficient transfer occurs with the frequency offsets along the diagonal, i.e. $f_H = f_C$, where f_H and f_C represent the frequency offsets for ^{1}H and ^{13}C, respectively, with maximal efficiency of ~ 0.73 (b, dashed line). Efficient transfer can also be established along the anti-diagonal by using other super-cycled phases (Fig. S1). The different transfer profiles can provide flexibility to excite parts of nuclei in correlations.

With the 2 kHz dipolar coupling, the bandwidths of SPRx-4$_1$ and SPRx-4$_3$ are ~ 750 Hz and ~ 520 Hz, respectively (Fig. S2). Owing to the frequency-selectivity, the ^{1}H polarization can be selectively transferred to the weak-coupled $^{13}C_1$, although ^{1}H is strongly-coupled to $^{13}C_2$ (Fig. 2b, d). SPRx-4_3 provides a higher transfer efficiency of $^{1}H \rightarrow ^{13}C_1$ (0.7) as it has better selectivity than SPRx-4_1. It should be noted that the bandwidths in SPR are proportional to the dipolar coupling constants[28]. For this reason, the bandwidths of SPRx will be broader for stronger dipolar couplings, which are common for spin pairs such as ^{1}H-^{19}F, ^{1}H-^{13}C, and ^{1}H-^{15}N.

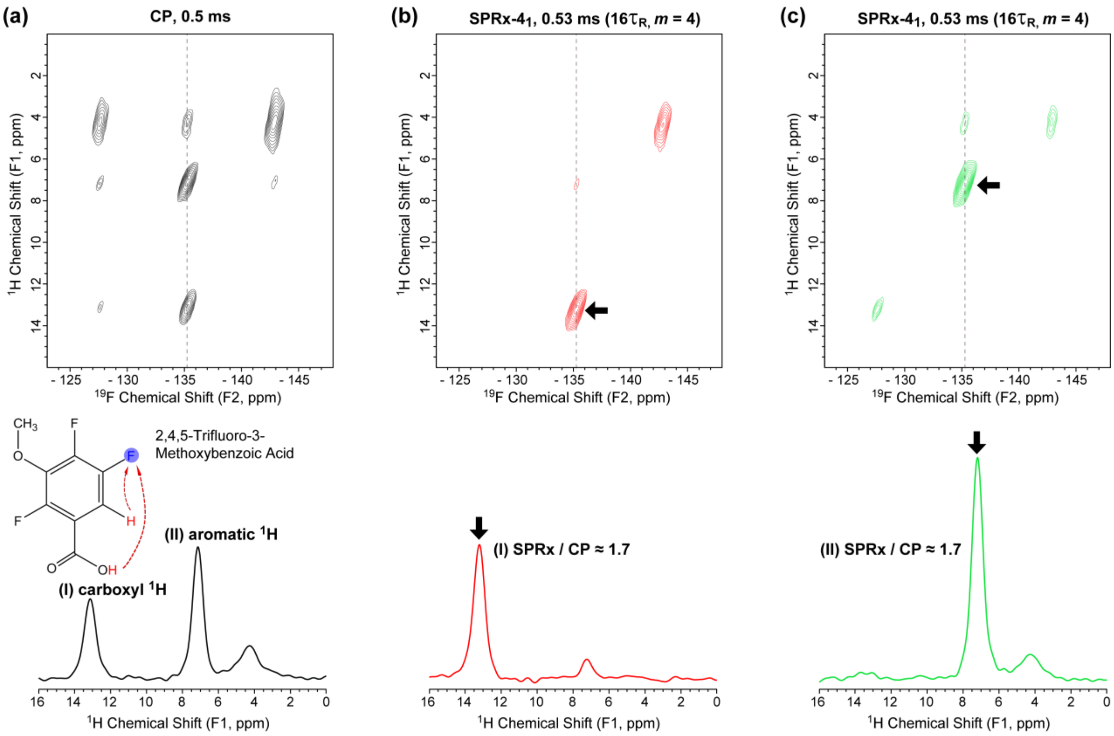

Figure 3 2D ^{1}H-^{19}F HETCOR (a) and FS-HETCOR (b, c) spectra (up) and 1D slices extracted along the dashed lines (bottom) of 2,4,5-trifluoro-3-methoxybenzoic acid (TMA) under 30 kHz MAS. FS-HETCOR experiments were performed using the sequence in Fig. 1b. The RF amplitudes of SPRx-4_1 are 60 kHz ($2\nu_R$) on both ^{1}H and ^{19}F. Red dashed arrows indicate the desired correlations in the molecular structure. Black arrows indicate the ^{1}H carrier transmitter during the SPRx-4_1 block (b, c). The ^{19}F carrier transmitter is set on F_5 (-135.2 ppm, blue) for all the experiments. The ^{1}H Larmor frequency is 500 MHz.

The ^{1}H-^{19}F FS-HETCOR experiments were performed on 2,4,5-trifluoro-3-methoxybenzoic acid (TMA) under 30 kHz MAS. SPRx-4_1 is used for selective ^{1}H-^{19}F polarization transfer as it can effectively overcome the interference from the relatively sizable ^{19}F chemical shift anisotropy. Figure 3a shows a regular 2D ^{1}H-^{19}F CP-based HETCOR spectrum, as a comparison. Since CP is non-selective, it is not surprising to observe multiple correlation peaks. Figure 3b and c show the 2D ^{1}H-^{19}F FS-HETCOR spectra using SPRx-4_1. Due to the frequency-selectivity of SPRx-4_1, the correlation peaks between F_5 and carboxyl ^{1}H (13.2 ppm, I) (b) and between F_5 and aromatic ^{1}H (7.1 ppm, II) (c) are both selectively enhanced by a factor of ~ 1.7. A few minor correlation peaks such as (7.1 ppm, -135.2 ppm) and (4.2 ppm, -135.2 ppm) (Fig. 2b and c) result from the transfer at the oscillating frequency (Fig. S2).

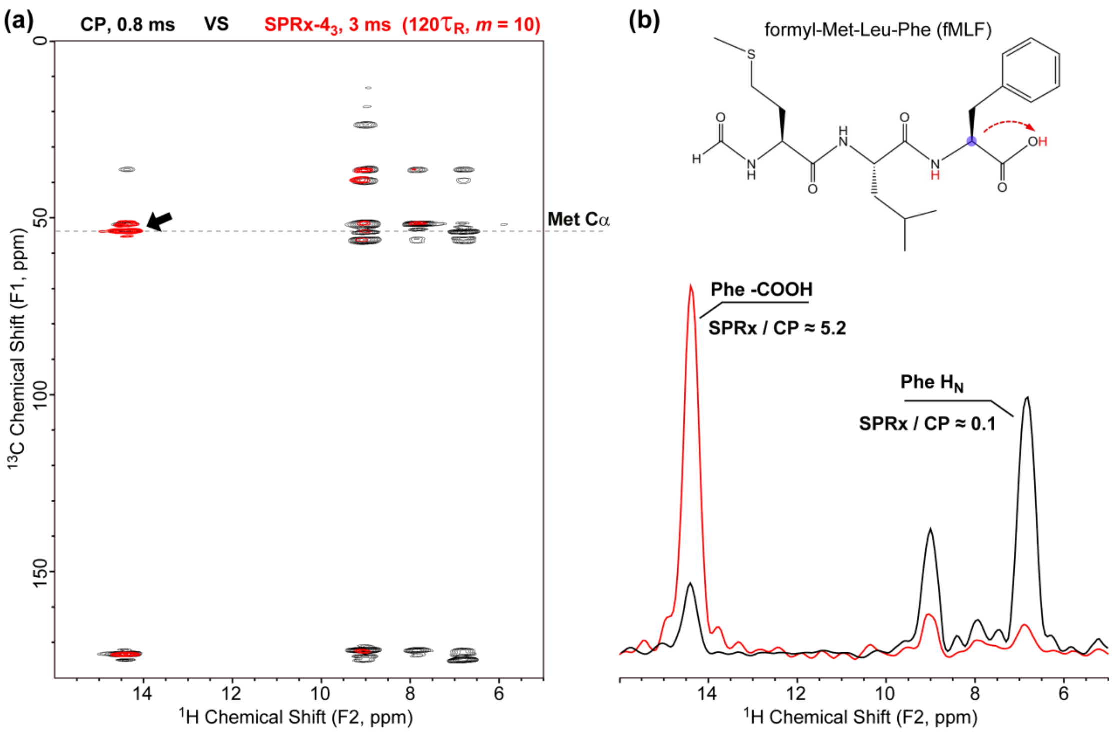

Figure 4 2D ^{13}C-^{1}H CP-HSQC (black) and FS-HETCOR (red) spectra (a) and 1D slices extracted along the dashed lines (b) of U-^{2}H, ^{13}C, ^{15}N labeled N-formyl-Met-Leu-Phe (fMLF) under 40 kHz MAS. The ^{1}H-detected FS-HETCOR experiment is performed using the sequence in Fig. 1c. The RF amplitudes of SPRx-4$_3$ are 26.7 kHz (0.667ν_R) on both ^{1}H and ^{13}C. The black arrow indicates the desired correlation peak between carbonyl ^{1}H (14.4 ppm) and Phe ^{13}Cα (54.3 ppm) (a) and the red dashed arrow indicates its origin in the molecular structure. The ^{1}H carrier transmitter is set at 10.3 ppm but moved to 14.4 ppm (carbonyl ^{1}H) during the SPRx-4$_3$ block. The ^{13}C carrier transmitter is set on Phe ^{13}Cα (54.3 ppm) for all the experiments. The ^{1}H Larmor frequency is 500 MHz.

The ^{1}H-detected FS-HETCOR experiments were carried out on U-^{2}H, ^{13}C, ^{15}N labeled N-formyl-Met-Leu-Phe (fMLF) under 40 kHz MAS. SPRx-4$_3$ is used for selective ^{1}H-^{13}C polarization transfer as it requires RF fields of 26.7 kHz (0.667ν_R). The low ^{13}C RF field can be readily achieved on fast MAS probes, which are optimized for ^{1}H detection and typically bear lower ^{13}C RF fields than probes optimized for ^{13}C detection.

Figure 4 shows the 2D ^{13}C-^{1}H CP-HSQC (black) and ^{1}H-detected FS-HETCOR (red) spectra. The cross peak between carbonyl ^{1}H (14.4 ppm) and Phe ^{13}Cα (54.3 ppm) is the correlation of interest as indicated by the arrow (Fig. 4a). In CP-HSQC, Phe $^{13}C\alpha$ is polarized mainly to the close Phe ^1H_N (6.8 ppm) but little to the remote Phe carboxylic ^1H (Fig. 4b, black). On the contrary, in the ^1H-detected FS-HETCOR, by using the frequency-selectivity of SPRx-4_3, the desired correlation peak between Phe $^{13}C\alpha$ and the carboxylic ^1H is selectively enhanced by a factor of ~ 5.2. Meanwhile, the unwanted correlation peak between Phe $^{13}C\alpha$ and ^1H_N is reduced to 10%. The enhancement of peaks of interest and the reduction of unwanted ones clearly verify the efficacy of frequency-selectivity of SPRx-N_n.

It is worth noting that the SPRx-4_1 and SPRx-4_3 are taken as examples to demonstrate their roles in FS-HETCOR experiments. They are demonstrated only under 30-40 kHz MAS restricted by our hardware capability. More representative SPRx-N_n are given in Table S2, which shall be applicable at arbitrary MAS rates, from relatively slow to ultrafast MAS. Besides, FS-HETCOR will benefit more from magnetic fields stronger than 11.25 T (^1H 500 MHz) used in this study, which increase the chemical shift dispersion in frequency units (Hz)[48-49].

Conclusions

In conclusion, we proposed novel FS-HETCOR experiments based on a new frequency-selective recoupling technique SPRx-N_n, aiming to enhance the heteronuclear correlations of interest by utilizing their distinct resonance frequencies. The ^1H-^{19}F and ^1H-^{13}C correlation experiments under 30-40 kHz MAS demonstrate that, compared to regular CP-based HETCOR, FS-HETCOR can selectively enhance the desired heteronuclear correlations by a factor of up to 5 and suppress the unwanted ones to 10%. It is thus anticipated to facilitate the observation of long-range correlations, which are usually truncated by short-range correlations in routine experiments. FS-HETCOR achieves the frequency-selectivity without any selective pulses and is extremely simple to set up. We believe that the method will enhance the ability of solid-state NMR to probe heteronuclear structural information. Future studies can be carried out in two directions. First of all, experiments with better frequency-selectivity can be performed on low-γ 1/2 spin pairs, e.g. ^{13}C-^{15}N, ^{13}C-^{31}P, and ^{13}C-^{29}Si, which have weaker dipolar couplings than ^1H-^{19}F and ^1H-^{13}C investigated in this study. Secondly, constant-time (CT) FS-HETCOR experiments can also be implemented following the means of homonuclear experiments[30, 50-52] so that heteronuclear distances can be measured quantitatively. Relevant work is underway.

Conflict of interest

The authors declare no conflict of interest.

Acknowledgments

This work was supported by grants from the National Natural Science Foundation of China (22074153, 21775161, 31770798, and 21927801), the National Key R&D Program of China (2017YFA0505400), and the Chinese Academy of Sciences (to Z. Z. and J. Y.). We

thank Dr. Mingyue Li for helping with preliminary experiments.

References

1. Maudsley, A. A.; Muller, L.; Ernst, R. R. Cross-Correlation of Spin-Decoupled NMR Spectra by Heteronuclear 2-Dimensional Spectroscopy. *J. Magn. Reson.* **1977,** *28* (3), 463-469.
2. Bodenhausen, G.; Ruben, D. J. Natural Abundance N-15 NMR by Enhanced Heteronuclear Spectroscopy. *Chem. Phys. Lett.* **1980,** *69* (1), 185-189.
3. Caravatti, P.; Bodenhausen, G.; Ernst, R. R. Heteronuclear Solid-state Correlation Spectroscopy. *Chem. Phys. Lett.* **1982,** *89* (5), 363-367.
4. Cavadini, S.; Lupulescu, A.; Antonijevic, S.; Bodenhausen, G. Nitrogen-14 NMR spectroscopy using residual dipolar splittings in solids. *J. Am. Chem. Soc.* **2006,** *128* (24), 7706-7707.
5. Gan, Z. Measuring amide nitrogen quadrupolar coupling by high-resolution N-14/C-13 NMR correlation under magic-angle spinning. *J. Am. Chem. Soc.* **2006,** *128* (18), 6040-6041.
6. Hing, A. W.; Vega, S.; Schaefer, J. Transferred-echo double-resonance NMR. *J. Magn. Reson.* **1992,** *96* (1), 205-209.
7. Michal, C. A.; Jelinski, L. W. REDOR 3D: Heteronuclear distance measurements in uniformly labeled and natural abundance solids. *J. Am. Chem. Soc.* **1997,** *119* (38), 9059-9060.
8. Hong, M.; Griffin, R. G. Resonance assignments for solid peptides by dipolar-mediated C-13/N-15 correlation solid-state NMR. *J. Am. Chem. Soc.* **1998,** *120* (28), 7113-7114.
9. Brinkmann, A.; Levitt, M. H. Symmetry principles in the nuclear magnetic resonance of spinning solids: Heteronuclear recoupling by generalized Hartmann-Hahn sequences. *J. Chem. Phys.* **2001,** *115* (1), 357-384.
10. Jaroniec, C. P.; Filip, C.; Griffin, R. G. 3D TEDOR NMR experiments for the simultaneous measurement of multiple carbon-nitrogen distances in uniformly C-13, N-15-labeled solids. *J. Am. Chem. Soc.* **2002,** *124* (36), 10728-10742.
11. Zhao, X.; Hoffbauer, W.; Gunne, J.; Levitt, M. H. Heteronuclear polarization transfer by symmetry-based recoupling sequences in solid-state NMR. *Solid State Nucl. Magn. Reson.* **2004,** *26* (2), 57-64.
12. Brinkmann, A.; Kentgens, A. P. M. Proton-selective O-17-H-1 distance measurements in fast magic-angle-spinning solid-state NMR spectroscopy for the determination of hydrogen bond lengths. *J. Am. Chem. Soc.* **2006,** *128* (46), 14758-14759.
13. Jain, S.; Bjerring, M.; Nielsen, N. C. Efficient and Robust Heteronuclear Cross-Polarization for High-Speed-Spinning Biological Solid-State NMR Spectroscopy. *J. Phys. Chem. Lett.* **2012,** *3* (6), 703-708.
14. Zhang, Z. F.; Chen, Y. K.; Yang, J. Band-selective heteronuclear dipolar recoupling with

dual back-to-back pulses in rotating solids. *J. Magn. Reson.* **2016,** *272*, 46-52.

15. Zhang, Z. F.; Li, J. P.; Chen, Y. K.; Xie, H. Y.; Yang, J. A robust heteronuclear dipolar recoupling method comparable to TEDOR for proteins in magic-angle spinning solid-state NMR. *J. Magn. Reson.* **2017,** *285*, 79-85.

16. Liang, L. X.; Ji, Y.; Zhao, Z. C.; Quinn, C. M.; Han, X. W.; Bao, X. H.; Polenova, T.; Hou, G. J. Accurate heteronuclear distance measurements at all magic-angle spinning frequencies in solid-state NMR spectroscopy. *Chem. Sci.* **2021,** *12* (34), 11554-11564.

17. Nimerovsky, E.; Xue, K.; Movellan, K. T.; Andreas, L. B. Heteronuclear and homonuclear radio-frequency-driven recoupling. *Magn. Reson.* **2021,** *2* (1), 343-353.

18. Pines, A.; Gibby, M. G.; Waugh, J. S. Proton-enhanced nmr of dilute spins in solids. *J. Chem. Phys.* **1973,** *59* (2), 569-590.

19. Metz, G.; Wu, X. L.; Smith, S. O. Ramped-amplitude cross polarization in magic-angle spinning NMR. *J. Magn. Reson. Ser. A* **1994,** *110* (2), 219-227.

20. Hediger, S.; Meier, B. H.; Ernst, R. R. Adiabatic passage Hartmann-Hahn cross polarization in NMR under magic angle sample spinning. *Chem. Phys. Lett.* **1995,** *240* (5-6), 449-456.

21. Baldus, M.; Petkova, A. T.; Herzfeld, J.; Griffin, R. G. Cross polarization in the tilted frame: assignment and spectral simplification in heteronuclear spin systems. *Mol. Phys.* **1998,** *95* (6), 1197-1207.

22. Laage, S.; Marchetti, A.; Sein, J.; Pierattelli, R.; Sass, H. J.; Grzesiek, S.; Lesage, A.; Pintacuda, G.; Emsley, L. Band-Selective H-1-C-13 Cross-Polarization in Fast Magic Angle Spinning Solid-State NMR Spectroscopy. *J. Am. Chem. Soc.* **2008,** *130* (51), 17216-17217.

23. Demers, J. P.; Vijayan, V.; Becker, S.; Lange, A. Tailored low-power cross-polarization under fast magic-angle spinning. *J. Magn. Reson.* **2010,** *205* (2), 216-223.

24. Reif, B.; Ashbrook, S. E.; Emsley, L.; Hong, M. Solid-state NMR spectroscopy. *Nat. Rev. Methods Primers* **2021,** *1* (1), 2.

25. Lu, X. Y.; Skomski, D.; Thompson, K. C.; McNevin, M. J.; Xu, W.; Su, Y. Three-Dimensional NMR Spectroscopy of Fluorinated Pharmaceutical Solids under Ultrafast Magic Angle Spinning. *Anal. Chem.* **2019,** *91* (9), 6217-6224.

26. Bayro, M. J.; Huber, M.; Ramachandran, R.; Davenport, T. C.; Meier, B. H.; Ernst, M.; Griffin, R. G. Dipolar truncation in magic-angle spinning NMR recoupling experiments. *J. Chem. Phys.* **2009,** *130* (11), 114506.

27. Zhang, Z. F.; Oss, A.; Org, M. L.; Samoson, A.; Li, M. Y.; Tan, H.; Su, Y. C.; Yang, J. Selectively Enhanced H-1-H-1 Correlations in Proton-Detected Solid-State NMR under Ultrafast MAS Conditions. *J. Phys. Chem. Lett.* **2020,** *11* (19), 8077-8083.

28. Xiao, H.; Zhang, Z. F.; Yang, J. Theory of frequency-selective homonuclear dipolar recoupling in solid-state NMR. *J. Chem. Phys.* **2021,** *155* (17), 174105.

29. Jain, M. G.; Lalli, D.; Stanek, J.; Gowda, C.; Prakash, S.; Schwarzer, T. S.; Schubeis, T.; Castiglione, K.; Andreas, L. B.; Madhu, P. K.; Pintacuda, G.; Agarwal, V. Selective H-1-H-1 Distance Restraints in Fully Protonated Proteins by Very Fast Magic-Angle Spinning Solid-State NMR. *J. Phys. Chem. Lett.* **2017,** *8* (11), 2399-2405.
30. Duong, N. T.; Raran-Kurussi, S.; Nishiyama, Y.; Agarwal, V. Quantitative H-1-H-1 Distances in Protonated Solids by Frequency-Selective Recoupling at Fast Magic Angle Spinning NMR. *J. Phys. Chem. Lett.* **2018,** *9* (20), 5948-5954.
31. Potnuru, L. R.; Duong, N. T.; Sasank, B.; Raran-Kurussi, S.; Nishiyama, Y.; Agarwal, V. Selective 1H-1H recoupling via symmetry sequences in fully protonated samples at fast magic angle spinning. *J. Magn. Reson.* **2021,** *328*, 107004-107004.
32. Bennett, A. E.; Becerra, L. R.; Griffin, R. G. Frequency-Selective Heteronuclear Recoupling in Rotating Solids. *J. Chem. Phys.* **1994,** *100* (2), 812-814.
33. Traaseth, N. J.; Veglia, G. Frequency-selective heteronuclear dephasing and selective carbonyl labeling to deconvolute crowded spectra of membrane proteins by magic angle spinning NMR. *J. Magn. Reson.* **2011,** *211* (1), 18-24.
34. Jaroniec, C. P.; Tounge, B. A.; Herzfeld, J.; Griffin, R. G. Frequency selective heteronuclear dipolar recoupling in rotating solids: Accurate C-13-N-15 distance measurements in uniformly C-13,N-15-labeled peptides. *J. Am. Chem. Soc.* **2001,** *123* (15), 3507-3519.
35. Trebosc, J.; Amoureux, J. P.; Wiench, J. W.; Pruski, M. Simultaneous frequency-selective solid-state NMR analysis of internuclear distances and through-bond connectivities in the presence of quadrupolar nuclei. *Chem. Phys. Lett.* **2003,** *374* (5-6), 432-438.
36. Bajaj, V. S.; Mak-Jurkauskas, M. L.; Belenky, M.; Herzfeld, J.; Griffin, R. G. DNP enhanced frequency-selective TEDOR experiments in bacteriorhodopsin. *J. Magn. Reson.* **2010,** *202* (1), 9-13.
37. Bodenhausen, G.; Freeman, R.; Morris, G. A. Simple Pulse Sequence for Selective Excitation in Fourier-Transform NMR. *J. Magn. Reson.* **1976,** *23* (1), 171-175.
38. Bauer, C.; Freeman, R.; Frenkiel, T.; Keeler, J.; Shaka, A. J. Gaussian Pulses. *J. Magn. Reson.* **1984,** *58* (3), 442-457.
39. Emsley, L.; Bodenhausen, G. Gaussian Pulse Cascades - New Analytical Functions for Rectangular Selective Inversion and in-phase Excitation in NMR. *Chem. Phys. Lett.* **1990,** *165* (6), 469-476.
40. Freeman, R. Shaped radiofrequency pulses in high resolution NMR. *Prog. Nucl. Magn. Reson. Spectrosc.* **1998,** *32*, 59-106.
41. Veshtort, M.; Griffin, R. G. High-performance selective excitation pulses for solid- and liquid-state NMR spectroscopy. *Chemphyschem* **2004,** *5* (6), 834-850.
42. Ishii, Y.; Tycko, R. Sensitivity enhancement in solid state N-15 NMR by indirect

detection with high-speed magic angle spinning. *J. Magn. Reson.* **2000,** *142* (1), 199-204.
43. Ishii, Y.; Yesinowski, J. P.; Tycko, R. Sensitivity enhancement in solid-state C-13 NMR of synthetic polymers and biopolymers by H-1 NMR detection with high-speed magic angle spinning. *J. Am. Chem. Soc.* **2001,** *123* (12), 2921-2922.
44. Chevelkov, V.; Rehbein, K.; Diehl, A.; Reif, B. Ultrahigh resolution in proton solid-state NMR spectroscopy at high levels of deuteration. *Angew. Chem. Int. Ed.* **2006,** *45* (23), 3878-3881.
45. Zhou, D. H.; Shah, G.; Cormos, M.; Mullen, C.; Sandoz, D.; Rienstra, C. M. Proton-detected solid-state NMR Spectroscopy of fully protonated proteins at 40 kHz magic-angle spinning. *J. Am. Chem. Soc.* **2007,** *129* (38), 11791-11801.
46. Zhou, D. H.; Shea, J. J.; Nieuwkoop, A. J.; Franks, W. T.; Wylie, B. J.; Mullen, C.; Sandoz, D.; Rienstra, C. M. Solid-rate protein-structure determination with proton-detected triple-resonance 3D magic-angle-spinning NMR spectroscopy. *Angew. Chem. Int. Ed.* **2007,** *46* (44), 8380-8383.
47. Bak, M.; Rasmussen, J. T.; Nielsen, N. C. SIMPSON: A general simulation program for solid-state NMR spectroscopy. *J. Magn. Reson.* **2000,** *147* (2), 296-330.
48. Callon, M.; Malar, A. A.; Pfister, S.; Rimal, V.; Weber, M. E.; Wiegand, T.; Zehnder, J.; Chavez, M.; Cadalbert, R.; Deb, R.; Dapp, A.; Fogeron, M. L.; Hunkeler, A.; Lecoq, L.; Torosyan, A.; Zyla, D.; Glockshuber, R.; Jonas, S.; Nassal, M.; Ernst, M.; Bockmann, A.; Meier, B. H. Biomolecular solid-state NMR spectroscopy at 1200 MHz: the gain in resolution. *J. Biomol. NMR* **2021,** *75* (6-7), 255-272.
49. Nimerovsky, E.; Movellan, K. T.; Zhang, X. C.; Forster, M. C.; Najbauer, E.; Xue, K.; Dervisoglu, R.; Giller, K.; Griesinger, C.; Becker, S.; Andreas, L. B. Proton Detected Solid-State NMR of Membrane Proteins at 28 Tesla (1.2 GHz) and 100 kHz Magic-Angle Spinning. *Biomolecules* **2021,** *11* (5), 18.
50. Paravastu, A. K.; Tycko, R. Frequency-selective homonuclear dipolar recoupling in solid state NMR. *J. Chem. Phys.* **2006,** *124* (19), 194303.
51. Tycko, R. Symmetry-based constant-time homonuclear dipolar recoupling in solid state NMR. *J. Chem. Phys.* **2007,** *126* (6), 064506.
52. Hu, K.-N.; Qiang, W.; Bermejo, G. A.; Schwieters, C. D.; Tycko, R. Restraints on backbone conformations in solid state NMR studies of uniformly labeled proteins from quantitative amide N-15-N-15 and carbonyl C-13-C-13 dipolar recoupling data. *J. Magn. Reson.* **2012,** *218*, 115-127.